

# IOWA STATE UNIVERSITY

## Digital Repository

---

Chemical and Biological Engineering  
Publications

Chemical and Biological Engineering

---

3-2016

## Fast pyrolysis of glucose-based carbohydrates with added NaCl part 1: Experiments and development of a mechanistic model

Xiaowei Zhou  
*Northwestern University*

Heather B. Mayes  
*Northwestern University*

Linda J. Broadbelt  
*Northwestern University*

*See next page for additional authors*

Follow this and additional works at: [https://lib.dr.iastate.edu/cbe\\_pubs](https://lib.dr.iastate.edu/cbe_pubs)



Part of the [Biochemical and Biomolecular Engineering Commons](#), and the [Catalysis and Reaction Engineering Commons](#)

The complete bibliographic information for this item can be found at [https://lib.dr.iastate.edu/cbe\\_pubs/421](https://lib.dr.iastate.edu/cbe_pubs/421). For information on how to cite this item, please visit <http://lib.dr.iastate.edu/howtocite.html>.

---

## Fast pyrolysis of glucose-based carbohydrates with added NaCl part 1: Experiments and development of a mechanistic model

### Abstract

Sodium ions, one of the natural inorganic constituents in lignocellulosic biomass, significantly alter pyrolysis behavior and resulting chemical speciation. Here, experiments were conducted using a micropyrolyzer to investigate the catalytic effects of NaCl on fast pyrolysis of glucose-based carbohydrates (glucose, cellobiose, maltohexaose, and cellulose), and on a major product of cellulose pyrolysis, levoglucosan (LVG). A mechanistic model that addressed the significant catalytic effects of NaCl on the product distribution was developed. The model incorporated interactions of Na<sup>+</sup> with cellulosic chains and low molecular weight species, reactions mediated by Na<sup>+</sup> including dehydration, cyclic/Grob fragmentation, ring-opening/closing, isomerization, and char formation, and a degradation network of LVG in the presence of Na<sup>+</sup>. Rate coefficients of elementary steps were specified based on Arrhenius parameters. The mechanistic model for cellulose included 768 reactions of 222 species, which included 252 reactions of 150 species comprising the mechanistic model of glucose decomposition in the presence of NaCl.

### Keywords

fast pyrolysis, reaction mechanism, kinetics, mechanistic modeling, sodium chloride

### Disciplines

Biochemical and Biomolecular Engineering | Catalysis and Reaction Engineering

### Comments

This is the peer reviewed version of the following article: Zhou, Xiaowei, Heather B. Mayes, Linda J. Broadbelt, Michael W. Nolte, and Brent H. Shanks. "Fast pyrolysis of glucose-based carbohydrates with added NaCl part 1: Experiments and development of a mechanistic model." *AIChE Journal* 62, no. 3 (2016): 766-777, which has been published in final form at DOI: [10.1002/aic.15106](https://doi.org/10.1002/aic.15106). This article may be used for non-commercial purposes in accordance with Wiley Terms and Conditions for Use of Self-Archived Versions

### Authors

Xiaowei Zhou, Heather B. Mayes, Linda J. Broadbelt, Michael W. Nolte, and Brent H. Shanks

# Fast Pyrolysis of Glucose-Based Carbohydrates with Added NaCl Part 1: Experiments and Development of a Mechanistic Model<sup>‡</sup>

**Xiaowei Zhou**

Dept. of Chemical and Biological Engineering, Northwestern University, 2145 Sheridan Road,  
Evanston, Illinois 60208, United States

**Michael W. Nolte**

Dept. of Chemical and Biological Engineering, Iowa State University, 2119 Sweeney Hall,  
Ames, Iowa 50011, United States

**Heather B. Mayes**

Dept. of Chemical and Biological Engineering, Northwestern University, 2145 Sheridan Road,  
Evanston, Illinois 60208, United States

**Brent H. Shanks**

Dept. of Chemical and Biological Engineering, Iowa State University, 2119 Sweeney Hall,  
Ames, Iowa 50011, United States

Center for Biorenewable Chemicals (CBiRC), Iowa State University, 1140 Biorenewables  
Research Laboratory Building, Ames, Iowa 50011, United States

**Linda J. Broadbelt\***

Dept. of Chemical and Biological Engineering, Northwestern University, 2145 Sheridan Road,  
Evanston, Illinois 60208, United States

---

<sup>‡</sup> Supporting Information may be found in the online version of this article.

\*Correspondence concerning this article should be addressed to B. H. Shanks at [bshanks@iastate.edu](mailto:bshanks@iastate.edu) and L. J. Broadbelt at [broadbelt@northwestern.edu](mailto:broadbelt@northwestern.edu)

This contribution was identified by Richard West (Northeastern University) as the Best Presentation in the session “Reaction Path Analysis I” of the 2014 AIChE Annual Meeting in Atlanta, GA.

**This article has been accepted for publication and undergone full peer review but has not been through the copyediting, typesetting, pagination and proofreading process which may lead to differences between this version and the Version of Record. Please cite this article as doi: 10.1002/aic.15106**

© 2015 American Institute of Chemical Engineers (AIChE)

Received: May 15, 2015; Revised: Oct 10, 2015; Accepted: Nov 12, 2015

This article is protected by copyright. All rights reserved.

## Abstract

Sodium ions, one of the natural inorganic constituents in lignocellulosic biomass, significantly alter pyrolysis behavior and resulting chemical speciation. Here, experiments were conducted using a micropyrolyzer to investigate the catalytic effects of NaCl on fast pyrolysis of glucose-based carbohydrates (glucose, cellobiose, maltohexaose and cellulose), and on a major product of cellulose pyrolysis, levoglucosan. A mechanistic model that addressed the significant catalytic effects of NaCl on the product distribution was developed. The model incorporated interactions of  $\text{Na}^+$  with cellulosic chains and low molecular weight species, reactions mediated by  $\text{Na}^+$  including dehydration, cyclic/Grob fragmentation, ring-opening/closing, isomerization, and char formation, and a degradation network of levoglucosan in the presence of  $\text{Na}^+$ . Rate coefficients of elementary steps were specified based on Arrhenius parameters. The mechanistic model for cellulose included 768 reactions of 222 species, which included 252 reactions of 150 species comprising the mechanistic model of glucose decomposition in the presence of NaCl.

**Keywords:** fast pyrolysis, reaction mechanism, kinetics, mechanistic modeling, sodium chloride.

## Introduction

Global warming and dwindling fossil fuel reserves spur interest in utilization of renewable energy. Renewable lignocellulosic biomass has been increasingly recognized as an alternative to petroleum for the production of transportation fuels and multiple commodity chemicals.<sup>1-5</sup> Fast pyrolysis is a promising thermochemical strategy that breaks down lignocellulosic biomass in the absence of oxygen at moderate temperature (typically 500 °C), yielding primarily a liquid product (bio-oil) that contains a range of low molecular weight compounds and can be catalytically upgraded to hydrocarbon fuel.<sup>6,7</sup>

Besides the three major constituents of cellulose, hemicelluloses, and lignin, biomass naturally contains minor amounts of mineral matter, which primarily consists of silicon, potassium, calcium, magnesium, sodium, phosphorus, and chlorine.<sup>8</sup> Although the total mineral content is typically less than 1 wt %, it has been demonstrated that these minerals, especially the alkali and alkaline earth metals, such as Na, K, Ca and Mg, even in small amounts, can have a profound effect on fast pyrolysis.<sup>8-11</sup> Additionally, it is costly to remove these inorganic metals from biomass before pyrolysis.<sup>12</sup>

NaCl is of special interest not only because it is one of the major indigenous inorganic salts in biomass, but also because it has been reported to have a similar influence as other alkali and alkaline earth metals on the product distribution from fast pyrolysis of biomass and cellulose.<sup>10,11,13-15</sup> Towards this end, extensive efforts have been devoted to experimentally studying the influence of naturally-occurring or artificially added NaCl on fast pyrolysis of cellulose, the most abundant constituent of biomass. Experiments showed that NaCl significantly reduced the yield of levoglucosan (*e.g.*, from 55 wt % to 9 wt % with addition of 0.05 wt % NaCl to cellulose) and simultaneously increased the yields of low molecular weight (LMW)

products.<sup>10,11,13,14,16</sup> The addition of NaCl accelerated the decomposition of cellulose, promoted the loss of water, and favored the formation of char and gaseous species during fast pyrolysis.<sup>13,17-19</sup>

Past experimental studies of the effects of inorganic salts on fast pyrolysis were often focused on the physical measurement and determination of global pyrolysis products and involved the use of a thermogravimetric analyzer (TGA),<sup>10,16-18,20</sup> which measures the overall decomposition and fails to provide a heating rate that is high enough for exploring the interacting physical mechanisms occurring under fast pyrolysis conditions. Additionally, few studies concern the influence of minerals on the detailed product speciation from fast pyrolysis. Particularly relevant work includes a study of the influence of varying amounts of inorganic salts (NaCl, KCl, MgCl<sub>2</sub>, CaCl<sub>2</sub>, Ca(OH)<sub>2</sub>, Ca(NO<sub>3</sub>)<sub>2</sub>, CaCO<sub>3</sub>, and CaHPO<sub>4</sub>) on the product speciation from pyrolysis of cellulose reported by Patwardhan et al. in 2010.<sup>11</sup> In their experiments, all the inorganic salts studied showed similar effects of greatly decreasing levoglucosan yield and accelerating the reactions that led to the formation of LMW species from cellulose as compared to those leading to anhydro sugars. However, recent experimental work on fast pyrolysis showed that more pyrolysis products could be more accurately identified and quantified.<sup>21-25</sup> Moreover, the influence of NaCl on other glucose-based carbohydrates such as maltohexaose and cellobiose has not been studied yet. Experimental data over a range of molecular weight would allow a better assessment of the influence of chain length on the product distribution from fast pyrolysis and rationalization of reaction intermediates and mechanisms involved. Moreover, a systematic study of product speciation arising from fast pyrolysis of glucose-based carbohydrates in the presence of NaCl would provide new understanding and insights into the mechanisms of fast pyrolysis of cellulose and real biomass.

Experimental studies on the evaporation of Na and Cl during fast pyrolysis of straw and NaCl-loaded samples revealed that the majority of Cl<sup>-</sup> was released below 400 °C, while negligible volatilization of Na<sup>+</sup> was observed even at 600 °C.<sup>17,26,27</sup> It has been postulated that sodium in the melt phase probably exists as ions bound to oxygen functionalities within the organic matrix during fast pyrolysis of biomass or cellulose.<sup>26,28-30</sup> Experimental work of Wu and co-workers on investigating reaction intermediates during fast pyrolysis of NaCl-loaded cellulose suggested that Na<sup>+</sup> interacted with ring oxygen atoms and catalyzed ring-opening, dehydration, decarboxylation and decarbonylation reactions, and hence, the destruction of sugar ring structures in cellulose pyrolysis was greatly promoted.<sup>28</sup> Yu et al.<sup>28</sup> also concluded that char formation was favored by the addition of NaCl in two ways. First, Na<sup>+</sup> suppressed the formation of volatiles and catalyzed the destruction of sugar ring structures via reactions such as dehydration and enhanced cross-linking and the conversion of the water-insoluble portion into char during pyrolysis. Second, Na<sup>+</sup> catalyzed the carbonization and repolymerization of water-soluble intermediates into char. Recent experiments of Liu et al.<sup>15</sup> revealed that cellulose dehydration was significantly catalyzed by Na<sup>+</sup> during isothermal pyrolysis. Nimlos et al.<sup>14</sup> reported that the presence of Na<sup>+</sup> in fast pyrolysis could lead to the formation of carbocations and oxonium ions as products, which are highly reactive and can serve as cross-linking agents and lead to the formation of char.

Computational chemistry calculations have also been performed to elucidate the mechanisms underlying the catalytic behavior and effects of NaCl on reactions relevant to fast pyrolysis of glucose and cellulose. Electronic structure calculations were performed by Nimlos et al. to investigate the 1,2-dehydration of alcohols as a model system for the dehydration of carbohydrates occurring in biomass/cellulose pyrolysis.<sup>14</sup> They revealed that the rates of 1,2-dehydration of alcohols with the addition of alkali metal cations and protons can be dramatically

increased, and the increase in rate was primarily due to a decrease in the energy barrier, which was caused by the stabilization of the transition state.<sup>14</sup> For example, the addition of  $\text{Na}^+$  decreased the activation energy ( $E_a$ ) from 67.4 to 60.0 kcal·mol<sup>-1</sup> and increased the reaction rate by a factor of 30 times for 1,2-dehydration of ethanol to ethylene. A density functional theory (DFT) study of Zhang and Liu on pyrolysis of  $\beta$ -D-glucopyranose discovered that  $\text{Na}^+$  can lower the energy barrier of dehydration reactions and accelerate the formation of small molecules.<sup>31</sup> Quantum chemical calculations of Mayes et al. revealed that dehydration of  $\beta$ -D-glucopyranose to levoglucosan-pyranose (LVG) and cyclic enols, dehydration of  $\beta$ -D-glucofuranose to levoglucosan-furanose, and dehydration of  $\beta$ -D-fructose to 5-hydroxymethylfurfural (5-HMF) can be affected by the presence of  $\text{Na}^+$  to differing degrees.<sup>25</sup> Mayes et al. also discovered that ring-opening of  $\beta$ -D-glucose to D-glucose and isomerization of D-glucose to D-fructose can also be facilitated by the presence of  $\text{Na}^+$ .<sup>25</sup>

These computational studies help to explain the catalytic effects of NaCl on fast pyrolysis and also provide kinetic parameters for the catalyzed reactions. While these results alone do not quantitatively rationalize experimentally observed product yields, they provide the necessary data to build a microkinetic model of the reaction chemistry, which can provide quantitative information on the rate of thermoconversion of carbohydrates and their resulting product distribution in the presence of NaCl under various operating conditions of fast pyrolysis.<sup>23,24,32,33</sup>

In the absence of mechanistic understanding, a previous kinetic model of the pyrolysis of cellulose and other carbohydrates in the presence of inorganic salts relied on global lumped schemes in which a correlation factor was employed to deal with the impact of inorganic salts on the overall yields of a small number of global lumped pyrolysis products. Specifically, Raveendran et al.<sup>8</sup> proposed a correlation in which the change in the total yield of volatile



products was expressed as a function of lignin content of biomass and the amounts of potassium and zinc. Such a model can not predict detailed product speciation and how it varies with pyrolysis conditions. A mechanistic model capturing individual elementary reactions would predict product speciation and be sensitive to differences in feedstocks and operating conditions, assisting in process optimization to produce target components with maximum value. Recently, the Broadbelt group developed detailed mechanistic models for fast pyrolysis of neat glucose-based carbohydrates, the results of which closely matched the experimental yields of various pyrolysis products over a wide range of temperatures and provided information about quantities based on mechanistic insight that was not accessible experimentally, such as the pyrolysis timescale, dynamic evolution of pyrolysis products, and the dominant reaction pathways for individual products.<sup>23,24,33</sup> However, the effects of NaCl on fast pyrolysis were not included.

Despite the past efforts of experimental investigation of operating conditions on fast pyrolysis product speciation, computational chemistry calculations to elucidate reaction mechanisms of model compounds, kinetic modeling using a lumping strategy, and mechanistic modeling of neat pyrolysis, a full mechanistic map of cellulose pyrolysis under the influence of NaCl and the quantification of the resulting product distribution are still not available. Towards this end, experiments and mechanistic modeling were conducted in this work to investigate the reaction mechanism and quantify the effects of NaCl on the product speciation from fast pyrolysis of glucose-based carbohydrates including glucose, cellobiose, maltohexaose and cellulose. In Part 1 of this study, we report on experiments of fast pyrolysis of glucose-based carbohydrates in the presence of NaCl at 500 °C that were conducted with a micropyrolyzer coupled to a gas chromatography–mass spectrometry (GC-MS)/flame ionization detector (FID) system. We also detail the development of a mechanistic model that incorporates the catalytic effects of NaCl on

pyrolysis species, reactions, and product distribution that was constructed for fast pyrolysis of glucose-based carbohydrates in the presence of NaCl. The experimental data were then used in Part 2 of this study to evaluate the quantitative and predictive performance of the mechanistic model, which was employed to identify and quantify dominant reaction pathways to different low molecular weight products and the critical role that inorganic components play.

## Experimental Section

### *Experimental materials*

Cellulose, in the form of microcrystalline powder of 50  $\mu\text{m}$  average particle size, was purchased from Sigma–Aldrich. The commercially available cellulose sample contained a negligible amount of mineral impurities<sup>11,34</sup> and was used as the pure cellulose in this work. The NaCl used in this work was purchased from Fischer Scientific as ACS grade with >99.5% purity. Cellulose samples were doped with NaCl at four concentrations ranging from 0.05 to 2.5 wt %. These weight percents were chosen to mimic those present in real biomass feedstocks. The appropriate amount of NaCl was dissolved in 10 mL methanol, and this solution was then added to 1 g of cellulose and stirred well to obtain a well-mixed slurry. The samples were dried in an oven at 40 °C *in vacuo* to obtain the NaCl-impregnated cellulose samples.

Maltohexaose, cellobiose, glucose, and levoglucosan with a sufficiently low amount of mineral impurities were purchased from Sigma–Aldrich and used as pure samples. NaCl-impregnated maltohexaose, cellobiose, glucose, and levoglucosan samples were prepared following the same procedure as NaCl-impregnated cellulose samples.

### *Pyrolyzer–GC–MS/FID experiments and product identification*

All experimental data were gathered using a Frontier Laboratories 2020 iS single-shot micropyrolyzer. Details on the operating method and quantification procedure can be found in

our previous work.<sup>23,24</sup> Briefly, 200–500  $\mu\text{g}$  of carbohydrate-salt mixture was loaded into a deactivated stainless steel sample cup. A preheated furnace temperature of 500  $^{\circ}\text{C}$  was used for every experiment. Separation of volatile compounds was achieved using a Bruker gas chromatograph (430-GC) fitted with a medium polarity capillary column. Products were identified using a mass spectrometer (MS) (Saturn 2000) and quantified using a FID. CO and CO<sub>2</sub> were quantified using an infrared De-Jaye gas analyzer. The yield of char was measured by weighing sample cups pre- and post pyrolysis using a Mettler Toledo microbalance  $\pm 1 \mu\text{g}$ .

### ***Experimental results***

The experimental purpose of this work is to investigate the effects of NaCl on chemical speciation resulting from fast pyrolysis of glucose-based carbohydrates and provide experimental data for mechanistic modeling. All the experiments in this study were carried out at 500  $^{\circ}\text{C}$ , and the final yields of various products from fast pyrolysis of glucose, cellobiose, maltohexaose, and cellulose over a wide range of NaCl concentrations are summarized in Tables S1–S4 (in the Supporting Information), respectively. Corresponding values of one standard deviation of the product yields for the triplicate runs are also given in Tables S1–S4. Note that data provided in Table S1 was presented in the Supporting Information of the study by Mayes et al.<sup>25</sup> of glucose decomposition with and without NaCl, but it is repeated in the Supporting Information for easier reference and comparison with other glucose-based carbohydrates. The concentrations of NaCl are based on the initial loading of a given glucose-based carbohydrate.

As shown in Tables S1–S4, a total of thirty-one compounds were identified from fast pyrolysis of neat/NaCl-impregnated glucose-based carbohydrates. There were also several products including compounds with a molecular weight of 86 g/mol and 102 g/mol that could not be definitively confirmed due to the unavailability of their pure standards. The quantitative yields of

pyrolysis products from fast pyrolysis of neat glucose-based carbohydrates have been reported in our previous work.<sup>23</sup> In this paper, product speciation arising from fast pyrolysis of glucose-based carbohydrates doped with varying amounts of NaCl was reported.

### ***Effect of NaCl on fast pyrolysis of glucose***

Table S1 summarizes the yields of pyrolysis products from fast pyrolysis of glucose in the presence of NaCl. As noted in our previous work<sup>25</sup>, it was intriguing that the same products are observed, but in different ratios without or with different amounts of NaCl. The magnitude of the effects of NaCl on glucose pyrolysis is more subtle than that observed for the other carbohydrates in this study.

While the increases in the yields of LVG and levoglucosan-furanose were within experimental error for an initial loading of 0.03 mmol NaCl/g of glucose, the yields of LVG and levoglucosan-furanose dropped from  $8.40 \pm 1.06$  to  $5.36 \pm 0.20$  wt % and  $4.28 \pm 0.50$  to  $2.31 \pm 0.19$  wt %, respectively, as the NaCl concentration was increased to 0.08 mmol/g, and then changed by a smaller amount as NaCl concentration further increased. The yield of 5-HMF underwent an initial increase from  $4.93 \pm 0.09$  to  $6.27 \pm 0.17$  wt % followed by a decrease to  $5.55 \pm 0.82$  wt %, then reached a maximum of  $6.47 \pm 0.48$  wt %, and then decreased again to  $4.61 \pm 0.24$  wt % as the addition of NaCl increased from 0 to 0.34 mmol NaCl/g of glucose. The yield of methyl glyoxal showed a similar variation as 5-HMF with the addition of NaCl. The formation of gaseous species, CO and CO<sub>2</sub>, char, and H<sub>2</sub>O was facilitated as the NaCl concentration increased. The formation of small aldehydes and other low molecular weight products (LMWPs) often involves retro-aldol, retro Diels–Alder, or tautomerization reactions.<sup>23,24</sup> With increasing amounts of NaCl doped into glucose, the yield of formaldehyde was first slightly reduced then sharply increased to its maximum, and then slightly decreased again, while the yields of

acetaldehyde and acetol consistently decreased. The yield of glycolaldehyde (GA) decreased from  $5.21 \pm 0.46$  to  $3.18 \pm 1.00$  wt % in the presence of 0.16 mmol NaCl/ g of glucose; however, greater amounts of NaCl led to an increase in this yield to  $4.64 \pm 0.29$  wt %.

#### ***Effect of NaCl on fast pyrolysis of cellobiose***

Table S2 presents the yields of products from fast pyrolysis of cellobiose with the addition of NaCl ranging from 0 to 0.21 mmol/g. The effects of NaCl on cellobiose were more pronounced than for glucose. The yield of LVG consistently decreased with increasing amounts of NaCl doped. The yields of 5-HMF, levoglucosenone, methyl glyoxal, acetaldehyde, and acetone increased monotonically, while the yield of GA decreased continuously from  $7.14 \pm 1.67$  to  $6.16 \pm 1.47$  wt %. Again, the yields of CO<sub>2</sub>, char, and H<sub>2</sub>O decreased slightly with an initial loading of 0.02 mmol NaCl/g of cellobiose, and then increased as the addition of NaCl increased, while the yield of CO increased monotonically with increasing NaCl loading. The yields of GA and LVG are higher from cellobiose pyrolysis than those from glucose pyrolysis, while the yields of other species such as 5-HMF, char, H<sub>2</sub>O, CO<sub>2</sub>, CO, methylglyoxal, and levoglucosenone are lower.

#### ***Effect of NaCl on fast pyrolysis of maltohexaose***

A stronger effect of NaCl on product speciation from fast pyrolysis of maltohexaose than that of cellobiose in the presence of NaCl was observed, as shown in Table S3. The yield of LVG was reduced from  $33.11 \pm 3.89$  to  $14.96 \pm 0.57$  wt %, and the yield of GA decreased from  $8.46 \pm 0.39$  to  $5.31 \pm 0.39$  wt % as the addition of NaCl increased from 0 to 0.30 mmol/g. The yields of small compounds such as formaldehyde, acetaldehyde, methanol, and acetol increased with the amount of NaCl added to maltohexaose, and the yields of CO<sub>2</sub> and char were also observed to increase monotonically from  $6.11 \pm 0.46$  to  $9.50 \pm 1.42$  wt % and  $5.51 \pm 0.79$  to  $7.78 \pm 3.24$  wt

%, respectively. The formation of CO and H<sub>2</sub>O was enhanced by the addition of NaCl to maltohexaose, and their maximum yields were reached in the presence of 0.01 and 0.18 mmol NaCl/g of maltohexaose, respectively.

### ***Effect of NaCl on fast pyrolysis of cellulose***

Table S4 summarizes the yields of products from fast pyrolysis of cellulose in the presence of NaCl at 500 °C. Similar to pyrolysis of glucose, cellobiose, and maltohexaose, the presence of NaCl in cellulose pyrolysis led to higher yields of LMW compounds, furan ring derivatives, non-condensable gas species, char, and H<sub>2</sub>O, and lower yields of anhydro sugars and dianhydro sugars, as compared to fast pyrolysis of neat cellulose.

For individual products, NaCl showed a more profound influence on altering yields as the chain length was increased from glucose, cellobiose, maltohexaose, to cellulose, with the most acute effect for cellulose. For example, declining profiles of LVG yield were experimentally observed in fast pyrolysis of all glucose-based carbohydrates as the amount of NaCl was increased. However, LVG yield dropped from  $54.50 \pm 1.33$  to  $8.52 \pm 0.20$  wt % for cellulose as compared to from  $33.11 \pm 3.89$  to  $14.96 \pm 0.57$  wt % for maltohexaose, from  $27.23 \pm 3.70$  to  $16.18 \pm 1.35$  wt % for cellobiose, and from  $8.10 \pm 1.47$  to  $5.32 \pm 0.87$  wt % for glucose. Unlike the decreasing trends with increasing addition of NaCl to glucose, cellobiose, and maltohexaose, an increase in GA yield from  $7.88 \pm 0.44$  to  $12.12 \pm 0.88$  and further to  $15.63 \pm 0.20$  wt % was observed when the addition of NaCl to cellulose increased from 0 to 0.01 mmol/g and then to 0.05 mmol/g. Further increase in the addition of NaCl reduced the formation of GA. As reported in our previous work<sup>23,24</sup>, decomposition of cellulosic chains via endchain initiation and depropagation contributes over 95% to the final yield of LVG, and GA directly formed from the cellulosic chains comprises more than 60% of its final yield from the fast pyrolysis of neat

cellulose. The observed decline in the yields of these two species with NaCl added suggests that the presence of NaCl has a significant impact on the formation of LVG and GA through the decomposition of cellulosic chains. 5-HMF was formed in lower yield in the presence of NaCl compared to that from neat cellulose, which was different from the trends of increasing yield of 5-HMF that was observed in fast pyrolysis of glucose, cellobiose, and maltohexaose as increased amounts of NaCl were doped. The yields of levoglucosan-furanose and dianhydroglucopyranose decreased from  $2.31 \pm 0.29$  to  $0.27 \pm 0.06$  wt % and from  $4.9 \pm 0.66$  to  $1.39 \pm 0.09$  wt %, respectively, even for an initial NaCl addition of 0.01 mmol/g of cellulose. Increasing yields of char, CO, and CO<sub>2</sub> from  $4.57 \pm 0.79$  to  $9.02 \pm 0.17$  wt %,  $1.84 \pm 0.18$  to  $2.77 \pm 0.18$  wt %, and  $3.57 \pm 1.22$  to  $7.63 \pm 0.30$  wt %, respectively, were observed for cellulose pyrolysis. The formation of formaldehyde, acetaldehyde, acetone, and acetol was also enhanced in the presence of NaCl.

As shown in Table S4, LVG is the most abundant product from fast pyrolysis of neat cellulose, accounting for  $54.50 \pm 1.33$  wt % in yield, while the presence of NaCl in as little as 0.05 mmol/g of cellulose pyrolysis sharply reduced the yield of LVG to less than 10.00 wt %. A similar effect of very small amounts of NaCl on decreasing the yield of LVG from fast pyrolysis of cellulose has been widely reported in the literature.<sup>10,11,13,16-18</sup> However, the underlying chemistry had yet to be rationalized.

#### ***Effect of NaCl on fast pyrolysis of levoglucosan***

As noted above, the presence of NaCl at a concentration as low as 0.05 mmol/g of cellulose sharply reduced the yield of LVG from  $54.50 \pm 1.33$  wt % to less than 10.00 wt %. There are two potential processes that LVG undergoes once it is formed from primary reactions during fast

pyrolysis: (1) LVG serves as an intermediate in the formation of other small compounds, (2) LVG vaporizes quickly and leaves the reaction zone as it is formed.<sup>34-39</sup>

Our previous work has revealed that the decrease in the yield of LVG from fast pyrolysis of neat cellulose at increasing temperatures was caused by the competing decomposition routes of cellulosic chains to give LVG, glucose, GA and other LMW species.<sup>23,24</sup> The decreasing yield as temperature was raised was not caused by the degradation of LVG because no degradation occurred to the LVG formed during fast pyrolysis of neat glucose-based carbohydrates or LVG as a reactant, due to the presence of a helium gas sweep in the experimental apparatus.<sup>23,24</sup> To determine whether inorganic salts would assist degradation of LVG, experiments of fast pyrolysis of LVG in the presence of different amounts of NaCl were conducted, and the results are summarized in Table S5 (in the Supporting Information).

As shown in Table S5, no degradation was observed for neat LVG as a reactant, which is consistent with our previous work<sup>23,24</sup> as well as that of Patwardhan et al.<sup>34</sup> Interestingly, fast pyrolysis of LVG in the presence of NaCl yielded a range of product species, indicating that NaCl does assist the decomposition of LVG during fast pyrolysis. The major products arising from LVG decomposition include dianhydroglucopyranose, GA, methylglyoxal, acetol, acetaldehyde, char, CO, CO<sub>2</sub> and water. The yields of GA and dianhydroglucopyranose increased from  $0.56 \pm 0.43$  to  $2.09 \pm 0.28$  wt % and  $0.13 \pm 0.08$  to  $1.08 \pm 1.09$  wt %, respectively, as the doped amount of NaCl increased from 0.19 to 0.56 mmol/g of LVG, and the weight ratio of GA to dianhydroglucopyranose decreased from 4.3 to 1.9. However, the weight ratio of GA to dianhydroglucopyranose for fast pyrolysis of glucose-based carbohydrates not only was much larger but also showed an increasing trend as the amount of doped NaCl increased. Specifically, the ratio increased from 12.7 to 22.5 for glucose, from 8.3 to 10 for



cellobiose, from 4.7 to 7.8 for maltohexaose, and from 8.7 to 34.5 for cellulose. These results indicate that the predominant pathways for the formation of LMW species from fast pyrolysis of glucose-based carbohydrates involve intermediates other than LVG, although there will clearly be a role for LVG-mediated pathways given that it is reactive in the presence of NaCl and is an intermediate of the pyrolysis of glucose-based carbohydrates.

As shown in Table S5, 90% and 76% mass closure was achieved for fast pyrolysis of levoglucosan with NaCl loadings of 0.19 mmol/g and 0.56 mmol/g, respectively. The unaccounted for mass was likely caused by a combination of the condensation of minor products such as oligomers in the transfer line between the pyrolysis reactor (500 °C) and the GC column (270–300 °C), non-quantified minor peaks in the chromatograph, and undetectable gases such as hydrogen and light hydrocarbons (such as CH<sub>4</sub>, C<sub>2</sub>H<sub>6</sub> and C<sub>3</sub>H<sub>8</sub>).

### **Mechanistic Modeling of the Effects of NaCl on Fast Pyrolysis**

In this section, we discuss building a mechanistic model that incorporates the effects of NaCl on the product distribution of fast pyrolysis of glucose-based carbohydrates that addresses the following questions: What kind of reactions can be affected by the presence of NaCl in fast pyrolysis? How does NaCl affect those reactions? How does the model include the catalytic effects of NaCl on fast pyrolysis at the mechanistic level? Can we have a single mechanistic model that captures the effects of NaCl on fast pyrolysis of a range of glucose-based carbohydrates?

As shown in the experimental section, the same chemical species were obtained in the presence of NaCl as those obtained from fast pyrolysis of pure glucose-based carbohydrates, but the relative yields of these pyrolysis products were different from the neat cases. Based on these observations, we hypothesized that the reactions occurring in fast pyrolysis of glucose-based

carbohydrates in the presence of NaCl follow the same mechanism as those taking place in fast pyrolysis of neat glucose-based carbohydrates, but with the kinetics altered.<sup>25</sup> In our previous work, we reported a detailed mechanistic model for fast pyrolysis of neat glucose-based carbohydrates, which included the decomposition of polymeric and oligomeric chains and reactions of glucose intermediates along with a range of LMW species.<sup>23,24</sup> Here we extend the model to incorporate the effects of NaCl on fast pyrolysis. As described in our mechanistic model for fast pyrolysis of neat glucose-based carbohydrates, decomposition reactions of cellulosic chains included initiation, depropagation, end-chain initiation, thermohydrolysis, dehydration, 1,2-dehydration, midchain dehydration, and retro Diels–Alder reactions, and reactions of LMW species included ring opening/closing, dehydration, 1,2-dehydration, isomerization, retro-aldol, retro Diels–Alder, cyclic/Grob fragmentation, enol-keto tautomerization, and char formation. All these reactions are applied here to describe the reactions of neutral species in fast pyrolysis.

The model was built based on the assumption that the catalytic effects of NaCl on fast pyrolysis of glucose-based carbohydrates and LVG relied on  $\text{Na}^+$ , an assumption supported by previous computational and experimental studies.<sup>30</sup> Moreover, Patwardhan et al.<sup>11</sup> and other researchers<sup>40,41</sup> reported that the cations had a much greater effect on the product distribution of fast pyrolysis of cellulose than the anions did. With NaCl present in fast pyrolysis of glucose-based carbohydrates at 500 °C in this study, chloride would be efficiently volatilized while sodium would stay in the melt phase, based on the experimental findings from the literature.<sup>14, 21, 22</sup> Furthermore,  $\text{Na}^+$  would be likely to bind with oxygen atoms in the reactive species.<sup>26,28-30</sup> In this work,  $\text{Na}^+$  ions were assumed to be able to bind with all the neutral species including polymeric chains and LMW species and form  $\text{Na}^+$ -complex species ( $\text{Na}^+$ -complexes). Once these

complexes are formed, they can undergo the same reactions as their neutral counterparts, but with different kinetics. Although quantum chemical calculations reveal specific interactions of  $\text{Na}^+$  ions with oxygen-containing carbohydrates, the specific geometries/structures of the  $\text{Na}^+$ -complexes were not required for the mechanistic model, although it was assumed that only one  $\text{Na}^+$  complexed at any instant with a given species. As reviewed in the Introduction, previous experimental and computational efforts have demonstrated that  $\text{Na}^+$  imparts catalytic effects on dehydration, ring-opening/ring-closing, the loss of water, char formation, etc. occurring in fast pyrolysis.<sup>13-15,17-19,25,28</sup> The specific reactions mediated by  $\text{Na}^+$  that are incorporated into the model to capture the effects of  $\text{Na}^+$  on fast pyrolysis are described in the following sections.

#### ***Modeling of $\text{Na}^+$ effects on decomposition of chain species***

Cellulose is a polysaccharide consisting of a linear chain of several hundreds to over ten thousand D-glucose units linked by glycosidic bonds.<sup>42</sup> In the modeling performed here, the initial degree of polymerization (DP) was set to 836, with an initial polydispersity of 2.25. While effects of initial DP on product distribution have been shown to be negligible beyond a DP value of 50, these initial values are consistent with those of the samples studied experimentally. The chains are assumed to not affect one another since it has been demonstrated that the thermal deconstruction products of pure cellulose are independent of degree of crystallinity.<sup>43</sup> Moreover, we have experimental evidence that our system is kinetically limited.<sup>43</sup> Given the relatively low concentrations of  $\text{Na}^+$  used, it is assumed that a given cellulose chain or its derived chains can have at most one  $\text{Na}^+$  bound (at a specific position, either at the end or in the middle). The position in the cellulosic chains where  $\text{Na}^+$  is bound is random, assuming an equal probability of  $\text{Na}^+$  binding with each monomer unit. Only reactions that take place at the monomer unit that is bound with  $\text{Na}^+$  can be affected by its presence. Furthermore, a simplification of multiplying the

pre-exponential factor of the reactions mediated by  $\text{Na}^+$  occurring at the mid-chain groups by a fit factor of 30 (sensitivity analysis on parameters presented in Part 2 of this work) to mimic the average number of catalytic sites within the polymeric chain species. As described in our previous model for fast pyrolysis of neat glucose-based carbohydrates, decomposition of the cellulosic chains can proceed via initiation, depropagation, end-chain initiation, thermohydrolysis, dehydration, 1,2-dehydration, midchain dehydration, and retro Diels–Alder.<sup>23,24</sup> Among these reactions, dehydration (reactions V and X) (see Schemes S1–S2 in the Supporting Information for the Roman numeral reactions), 1,2-dehydration (reactions VI and viii), and midchain dehydration (reactions i and iv) are the reactions that can be catalyzed by  $\text{Na}^+$ , which shows a negligible effect on the other reaction classes. In this work, it further assumes that the monomer unit that is bound with  $\text{Na}^+$  can only undergo these three dehydration reactions, while other monomer units of the  $\text{Na}^+$ -complex chains can still undergo all the decomposition reactions as the neutral chains, but with the reaction probability slightly changed because one unit is removed from doing the neutral chemistry.

Scheme 1 shows a representative example of how the effect of  $\text{Na}^+$  on decomposition of the chains is explicitly included in the model. For fast pyrolysis of cellulose, neutral cellulosic chains can undergo initiation to give a non-reducing-end (NR-end) chain and levoglucosan-end (LVG-end) chain, which undergoes depropagation to give a LVG-end chain and a molecule of LVG. At the same time, neutral cellulosic chains can also undergo dehydration to form chains with a dehydrated midgroup. In the presence of  $\text{Na}^+$ , each cellulose chain, NR-end chain, LVG-end chain, and dehydrated-midgroup chain can bind with one  $\text{Na}^+$  and form their corresponding  $\text{Na}^+$ -complex chains. Cellulose- $\text{Na}^+$  can undergo midchain dehydration catalyzed by  $\text{Na}^+$  to give a molecule of water and an  $\text{Na}^+$ -complex chain with a dehydrated-midgroup, which can undergo

unbinding to release  $\text{Na}^+$  with the concomitant formation of a neutral dehydrated-midgroup. However, midchain dehydration of  $\text{Na}^+$ -complex chains is 90 times (specification of rate parameters discussed in a later section and sensitivity analysis on parameters presented in Part 2 of this work) as fast at 500 °C as that of neutral chains due to the catalytic effects of  $\text{Na}^+$  on dehydration, and a fit factor of 30 was used to address the average number of catalytic sites on midgroups of cellulose. Meanwhile,  $\text{Na}^+$ -complex cellulose chains can also undergo an initiation reaction with a slightly lower reaction probability due to one fewer monomer unit being available for initiation to take place. A factor expressed as  $\exp(-1.5/X_n)$ , where  $X_n$  is the chain length, was used in the model to account for the change in the reaction probability. Similarly,  $\text{Na}^+$  binds with a neutral LVG-end chain and forms a  $\text{Na}^+$ -complex chain, LVG-end chain- $\text{Na}^+$ , which undergoes depropagation in the same way as neutral LVG-end chains but with a different reaction rate coefficient. The interactions (binding/unbinding) of  $\text{Na}^+$  with all the neutral chain species and the reactions of  $\text{Na}^+$ -complex chain species were incorporated in this model.

### ***Modeling of $\text{Na}^+$ effects on the reactions of LMW species***

Interactions of LMW species and reactions of  $\text{Na}^+$ -complex LMW species are also incorporated in the model. It is assumed that only one  $\text{Na}^+$  binds with a molecule of a neutral LMW species to form the corresponding  $\text{Na}^+$ -complex LMW species. Our previous model for neat carbohydrate pyrolysis includes the formation of 67 LMWPs via ring-opening/ring-closing, dehydration, 1,2-dehydration, isomerization, retro-aldol, retro Diels–Alder, cyclic/Grob fragmentation, enol-keto tautomerization, and char formation.<sup>23,24</sup> Among those reactions, dehydration, ring-opening/ring-closing, char formation and isomerization of D-glucose to D-fructose can be affected by the presence of  $\text{Na}^+$  as discussed above. Furthermore, past efforts showed that the addition of alkali ions to cellulose enhances the loss of water during pyrolysis.<sup>14</sup>

Cyclic/Grob fragmentation with involvement of the loss of water was thus assumed to be catalyzed by  $\text{Na}^+$  during fast pyrolysis.

Scheme 2 shows a representative example of the modeling approach to capture the effect of  $\text{Na}^+$  on the reactions of LMW species. Reactions (*e.g.*, dehydration) in which a sodium ion binds to a LMW species (*e.g.*, glucose and levoglucosan) to form a complex (*e.g.*, glucose- $\text{Na}^+$  and levoglucosan- $\text{Na}^+$ ) were included. The complexes can then undergo reactions analogous (*e.g.*, dehydration) to those in the absence of  $\text{Na}^+$ , albeit governed by different kinetic parameters<sup>25</sup> (*e.g.*,  $k_{\text{Na}^+}=50k_{\text{Neat}}$ ). Finally,  $\text{Na}^+$  unbinds from  $\text{Na}^+$ -complexes to form LMW products. The model includes the interactions of  $\text{Na}^+$  with all relevant species and corresponding  $\text{Na}^+$ -mediated reactions. These reactions included all the dehydration (reactions 1, 4, 8, 14, 22, 23, 24, 31, 32, 37, 38, 45, 52, 53, 55, 58, 60, 63, and 64) (see Schemes S3–S5 in the Supporting Information for reactions 1–99), ring-opening/ring-closing (reactions 2/3, 13/12, 21/20, 29/28, 36/35, 51/50, and 57/56), cyclic/Grob fragmentation (reactions 15, 30, 33, and 39), char formation (reactions 70–99), and isomerization of D-glucose to D-fructose (reaction 19).

### ***Modeling of levoglucosan degradation during fast pyrolysis in the presence of $\text{Na}^+$***

As shown in Table S5, dianhydro-glucopyranose, GA, methylglyoxal, acetol, acetaldehyde, char, CO,  $\text{CO}_2$  and water have been obtained as major products from fast pyrolysis of LVG in the presence of NaCl, while only LVG itself was detected in the absence of NaCl.

Many efforts have been devoted to studying the thermal degradation of LVG. Ronsse et al.<sup>44</sup> investigated the catalytic behavior of char in the decomposition of LVG using a micropyrolyzer system and revealed that metals, especially the alkali metals, rather than the fixed carbon in the char, catalyzed the decomposition of LVG, and the catalytic activity of char can be substantially reduced by acid washing. Kawamoto et al.<sup>45</sup> reported that inorganic salts greatly reduced the

yield of LVG and suggested pure cellulose should be used to avoid secondary reactions of LVG. Kawamoto et al.<sup>35</sup> hypothesized that LVG and polysaccharides existed as an equilibrium mixture in cellulose pyrolysis and proposed a global pyrolysis mechanism in which LVG formed from the decomposition of cellulose underwent two simultaneous reactions: (1) transformation into volatile LMW products, and (2) ring-opening polymerization into polysaccharides which eventually converted into char. A similar global kinetic scheme was proposed by Bai et al.<sup>36-38</sup>, in which LVG evaporated into the vapor phase or simultaneously acted as an intermediate to form oligosaccharides through polymerization. Oligosaccharides eventually dehydrated to char and light oxygenates.<sup>36-38</sup> Potential pathways of LVG decomposition via concerted reactions of dehydration, C-O bond breaking and C-C bond breaking have been reported in the literature.<sup>46-50</sup>

Based on these previous efforts and our experimental findings, a degradation mechanism of LVG in the presence of  $\text{Na}^+$  was proposed in this work, shown in Scheme 3. LVG can follow two competing routes during fast pyrolysis in the presence of NaCl. The first is volatilization (reaction 100) that takes LVG out of the melt phase into the vapor phase in which there is no degradation occurring to LVG. The other is LVG binding with  $\text{Na}^+$ , forming a complex of levoglucosan- $\text{Na}^+$  (reactions 101 and 102), which stays in the melt phase and undergoes further decomposition to form other LMW species. Reactions 103 and 104 represent the interconversion between levoglucosan- $\text{Na}^+$  and its acyclic isomer via ring-opening/ring-closing. The acyclic form of LVG can undergo retro-aldol and dehydration, followed by retro-aldol, enol-keto tautomerization, or decarbonylation to give LMW compounds such as GA, acetol, glyoxal, acetaldehyde, and acetone. Dehydration of levoglucosan- $\text{Na}^+$  (reactions 113, 114, and 115) gives water and dianhydro-glucopyranose. Levoglucosenone can be formed from 1,6:2,3-dianhydro-glucopyranose via pathway 59–60 as reported in our previous work.<sup>23,24</sup> Retro Diels–Alder of

1,6:3,4-dianhydro-glucopyranose (reaction 116) forms a cyclic C3 fragment and pyruvaldehyde which undergoes enol-keto tautomerization to form methyl glyoxal. Char, CO, CO<sub>2</sub>, H<sub>2</sub>O, and H<sub>2</sub> can be formed from the dehydrated species via char formation as described in our previous work.<sup>23,24</sup>

This degradation network described both the experimental observations of no degradation occurring to neat LVG and the formation of a range of LMW products from fast pyrolysis of LVG in the presence of NaCl at the mechanistic level.

***Unified mechanistic model for fast pyrolysis of glucose-based carbohydrates in the presence of NaCl***

The model developed here for fast pyrolysis of glucose-based carbohydrates is the first, to the best of our knowledge, that incorporates the effects of NaCl at the mechanistic level. It is built by incorporating the Na<sup>+</sup>-complex species formed from the interactions of Na<sup>+</sup> with neutral cellulosic chain species and LMW species and their reactions, as well as the degradation network of LVG in the presence of NaCl, combined with our previous mechanistic model for fast pyrolysis of neat glucose-based carbohydrates<sup>23,24</sup>. Table 1 gives the scaling of the model complexity without/with NaCl present in terms of the number of species and reactions. There is a sharp increase in the number of both species and reactions as the effects of Na<sup>+</sup> on fast pyrolysis are taken into account. For example, the number of species and reactions tracked by the model of glucose pyrolysis increased from 67 to 150 and from 96 to 252, respectively. The more than double the number of species being tracked by the model is attributed to the new species introduced by the decomposition of LVG in the presence of NaCl. The increase in the number of species and reactions from glucose to cellobiose is caused by the decomposition of disaccharide cellobiose to dimers and LMWPs. Note that there is a further increase in the number of species



and reactions from cellobiose to maltohexaose/cellulose, which is attributed to the decomposition of midgroup species of oligosaccharides/polysaccharides. Figure S1 (in the Supporting Information) lists the neutral species tracked in the model.

### ***Specification of rate parameters***

Specification of reasonable values of the rate parameters of the elementary steps in terms of the Arrhenius parameters,  $E_a$  and frequency factor ( $A$ ), is vital for the development of a kinetic model at the mechanistic level.<sup>51</sup> According to the reaction family approach<sup>32</sup>, kinetic parameters for retro-aldol, decarbonylation, enol-keto tautomerization, dehydration, retro Diels–Alder, and char formation, which have been reported in our model for fast pyrolysis of neat glucose-based carbohydrates<sup>23,24</sup>, are applied here to the reactions of neutral species that were introduced by the decomposition of LVG in the presence of NaCl. Kinetic parameters of the reactions of Na<sup>+</sup>-complexes are primarily derived from the quantum chemical calculations of Mayes et al.<sup>25</sup>. It should be pointed out, however, that  $A$  and  $E_a$  values estimated using quantum chemical calculations have uncertainties. For example, the mean unsigned error associated with the B3LYP hybrid functional for activation barriers has been shown to be 4.8 kcal/mol.<sup>52</sup> In this model,  $A$  values obtained by quantum chemical calculations in the literature were allowed to be adjusted by a factor ranging from 0.1 to 10 to address the uncertainty of calculated  $A$  values. Where data was unavailable, parameters were fitted to match product yields. Note that any fitting of kinetic parameters that was done in this work was performed against reactions mediated by Na<sup>+</sup> at 500 °C. The kinetic parameters of reactions of neat species that have been validated against experimental data of fast pyrolysis of glucose-based carbohydrates at temperatures ranging from 400–600 °C were adopted here without adjustment. Moreover, only experimental data from fast pyrolysis of glucose dosed with 0.03 mmol/g and 0.16 mmol/g and cellulose dosed

with 0.01 mmol/g and 0.21 mmol/g were used to fit parameters. All other experimental data from fast pyrolysis of glucose-based carbohydrates in the presence of NaCl were used for validation and evaluation of the model in Part 2 of this work.

In order to reduce the number of fitted kinetic parameters, the model used the same  $A$  or  $E_a$  values for a particular reaction family.<sup>32</sup> Rate parameters for the reactions that are newly incorporated into the mechanistic model to capture the effect of NaCl are summarized in Table 2, in which individual pre-exponential factors, activation energies, and corresponding reference sources are presented. The model used the same set of parameters for different feedstock carbohydrates (glucose, cellobiose, maltohexaose, and cellulose). Note that there are no chain species and associated reactions of chain species (numbered in Roman numerals) in fast pyrolysis of glucose. Therefore, only the kinetic parameters of reactions numbered in Arabic numerals were involved in modeling of fast pyrolysis of glucose.

Volatilization is a physical process. The volatilization rate of LVG in fast pyrolysis can be affected by many factors such as vapor pressure, temperature, surface area of LVG liquid, and LVG concentration in the melt phase. Without a more detailed description of the physical processes, the model used a fitted value of  $3.0 \text{ mol} \cdot \text{L}^{-1} \cdot \text{s}^{-1}$  for the volatilization rate of LVG. Armentrout and coworkers reported that, generally, there is no activation barrier in excess of the reaction endothermicity for the loss of the ligand from metal-ligand complexes.<sup>53-55</sup> Therefore, the model used  $0 \text{ kcal} \cdot \text{mol}^{-1}$  for the  $E_a$  of  $\text{Na}^+$  ion binding to neutral species. A frequency factor of  $1.0 \times 10^8 \text{ M}^{-1} \cdot \text{s}^{-1}$  is used for  $\text{Na}^+$  binding to all the neutral species.<sup>56</sup> Mayes et al.<sup>25</sup> estimated the Gibbs free energy change  $\Delta G_{773\text{K}}$  for the binding of isolated  $\text{Na}^+$  and glucose to form a  $\text{Na}^+$ -glucose complex to be  $10.0 \text{ kcal} \cdot \text{mol}^{-1}$ , with similar values found for many intermediates and products of glucose pyrolysis included in that study. The values relevant for the pyrolysis

environment are the difference in free energy as the ions migrate in the melt phase, which will not be as entropically unfavorable as calculated in the quantum chemical calculations for isolated species. Previous studies have demonstrated that cation-glucose binding is spontaneous and favorable.<sup>30</sup> Based on these considerations and a sensitivity analysis with the microkinetic model (see part 2 of this study for more details on sensitivity analysis of parameters), we utilized  $\Delta G = 3.0 \text{ kcal}\cdot\text{mol}^{-1}$  for binding of  $\text{Na}^+$  with all the species, from which the rate coefficient of unbinding was calculated to be  $7.05 \times 10^8 \text{ s}^{-1}$  at 773.15 K.

Kinetic parameters, especially  $E_a$  of the reactions catalyzed by  $\text{Na}^+$ , which were reported by Mayes et al.<sup>25</sup> based on their quantum chemical calculations, were utilized in this work. For example, the model utilized an  $E_a$  of  $47.4 \text{ kcal}\cdot\text{mol}^{-1}$ ,  $A$  of  $2.02 \times 10^{14} \text{ s}^{-1}$ , and reaction rate constant ratio ( $R_{\text{Na}^+}$ ) of 50 for dehydration of  $\beta$ -D-glucopyranose to LVG (reaction 1) in the presence of  $\text{Na}^+$ , based on the  $E_a$  of  $47.4 \text{ kcal}\cdot\text{mol}^{-1}$ ,  $A$  of  $4.2 \times 10^{14} \text{ s}^{-1}$  and  $R_{\text{Na}^+}$  of 52 reported by Mayes et al.<sup>25</sup> In this work, the reaction rate constant ratio ( $R_{\text{Na}^+}$ ) is defined as the ratio of the rate constant of the reaction in the presence of  $\text{Na}^+$  to that in the absence of  $\text{Na}^+$ . The same kinetic parameters of reaction 1 are applied to reaction V (Scheme S1; dehydration of the reducing end glucose monomer of a cellulose or oligomer chain).  $E_a$  of  $51.6 \text{ kcal}\cdot\text{mol}^{-1}$  for dehydration of  $\beta$ -D-furanose to 1,2-anhydro-furanose in the presence of  $\text{Na}^+$  (reaction 22), and  $E_a$  of  $38.3 \text{ kcal}\cdot\text{mol}^{-1}$  for dehydration of 1,2-anhydro-furanose to dianhydro-furanose (reaction 23) reported by Mayes et al.<sup>25</sup> were also applied here without adjustment. According to the reaction family approach<sup>32</sup>, kinetic parameters for dehydration of  $\beta$ -D-fructose to 5-HMF in the presence of  $\text{Na}^+$  were applied to similar dehydration reactions that led to the formation of other furans such as furfural and furanone.

Some parameters were adjusted within the limits of uncertainty typically associated with quantum chemical calculations. For instance, Mayes et al.<sup>25</sup> reported  $E_a$  of 59.0 kcal·mol<sup>-1</sup>,  $A$  of  $8.2 \times 10^{13}$  s<sup>-1</sup>, and  $R_{Na^+}$  of 6.7 for 1,2-dehydration of  $\beta$ -D-glucose to 1,2-anhydroglucosan (reaction 4) in the presence of Na<sup>+</sup>, for which the model used an  $E_a$  of 56.0 kcal·mol<sup>-1</sup>,  $A$  of  $2.31 \times 10^{15}$  s<sup>-1</sup>, and  $R_{Na^+}$  of 6.3. Kinetic parameters for reaction 4 were applied to reactions VI and viii according to the reaction family approach. The model used  $E_a$  of 49.2 kcal·mol<sup>-1</sup>,  $A$  of  $6.5 \times 10^{14}$  s<sup>-1</sup>, and  $R_{Na^+}$  of 2.1 for dehydration of  $\beta$ -D-glucofuranose to levoglucosan-furanose (reaction 14) mediated by Na<sup>+</sup>, for which  $E_a$  of 51.2 kcal·mol<sup>-1</sup>,  $A$  of  $1.4 \times 10^{14}$  s<sup>-1</sup>, and the same  $R_{Na^+}$  of 2.1 were reported by Mayes et al.<sup>25</sup>  $E_a$  of 50.5 kcal·mol<sup>-1</sup> and  $A$  of  $5.0 \times 10^{15}$  s<sup>-1</sup> were used for the dehydration of dianhydro-fructose to 5-HMF (reaction 24).

While the body of kinetic parameters for reactions mediated by Na<sup>+</sup> is expected to grow rapidly, even representative values were not available for all reaction families incorporated into the model. Therefore, a subset of the kinetic parameters was fitted to match experimental data. It has been widely reported that alkali and alkaline earth metal salts lower the activation energies of thermal decomposition, the overall reaction time and the decomposition temperature of fast pyrolysis.<sup>14,20,57-61</sup> In this work, kinetic parameters for reactions of Na<sup>+</sup>-complexes were fitted by lowering the activation energies of the corresponding reactions of the corresponding neutral species that were reported in our previous model<sup>23,24</sup>. The fitting procedure to obtain parameters that were not available in the literature was as follows. Firstly, the model gives the optimum reaction rate coefficients ( $k$ ) for the reactions mediated by Na<sup>+</sup> at 500 °C that minimize the difference between the experimental data and model results for products of fast pyrolysis of glucose and cellulose in the presence of NaCl. Then,  $E_a$  values of those reactions were calculated from  $k=A \cdot \exp(E_a/RT)$  by using the same values for  $A$  of the corresponding reactions without the

presence of  $\text{Na}^+$ , which have been reported in our previous model for fast pyrolysis of neat glucose-based carbohydrates.<sup>23, 24</sup> For example, midchain dehydration reactions of  $\text{Na}^+$ -complex chains were fitted to be 90 times as fast as those of neutral chains, and  $E_a$  was calculated to be  $53.1 \text{ kcal}\cdot\text{mol}^{-1}$ .  $E_a$  of  $25.9 \text{ kcal}\cdot\text{mol}^{-1}$  and  $R_{\text{Na}^+}$  of 3 were fitted for dehydration (reaction 45) of erythrose to form a compound with a molecular weight of  $102 \text{ g}\cdot\text{mol}^{-1}$ .  $E_a$  of  $47.8 \text{ kcal}\cdot\text{mol}^{-1}$  and  $R_{\text{Na}^+}$  of 5.7 were used for 1,2-dehydration of D-glucose (reactions 55, 63, 64, and 110).  $E_a$  of  $50.0 \text{ kcal}\cdot\text{mol}^{-1}$  and  $A$  of  $5.25 \times 10^{15} \text{ s}^{-1}$  were used in the model for dehydration of LVG to dianhydro- $\beta$ -D-glucopyranose (reactions 113, 114, and 115). Dehydration of propene (reaction 41) was assumed to not be catalyzed by  $\text{Na}^+$  since propene, which has a standard boiling point of  $-47.6^\circ\text{C}$ , would be volatilized into the gas phase once it is formed under the pyrolysis conditions of  $500^\circ\text{C}$  and using  $100 \text{ mL/min}$  of helium flow as a sweep.

As discussed above, it has been demonstrated that  $\text{Na}^+$  promotes the loss of water during fast pyrolysis of carbohydrates.<sup>14,15,31</sup> Cyclic/Grob fragmentation (reactions 15, 30, 33, and 39) that involves the loss of water would be promoted by  $\text{Na}^+$ . Therefore,  $E_a$  of cyclic/Grob fragmentation in the presence of  $\text{Na}^+$  was lowered to achieve a fitted  $R_{\text{Na}^+}$  of 10.0 in this model.

According to the quantum chemical calculations of Mayes et al.<sup>25</sup>, isomerization of D-glucose to D-fructose (reaction 19) mediated by  $\text{Na}^+$  is 4.5 times as fast as that in the neat case. Therefore, the model used an  $E_a$  of  $36.5 \text{ kcal}\cdot\text{mol}^{-1}$  as reported in their work, and the  $A$  was adjusted from  $2.6 \times 10^{12} \text{ s}^{-1}$  to  $1.50 \times 10^{12} \text{ s}^{-1}$  to maintain the same  $R_{\text{Na}^+}$  of 4.5.

Another type of reaction that can be affected by the presence of  $\text{Na}^+$  in fast pyrolysis is ring-opening/ring-closing. Kinetic parameters for ring-opening/ring-closing were from the quantum chemical calculations of Mayes et al.<sup>25</sup>  $E_a$  of  $46.3 \text{ kcal}\cdot\text{mol}^{-1}$  for ring-opening of  $\beta$ -D-glucopyranose to D-glucose (reaction 2) and  $E_a$  of  $37.8 \text{ kcal}\cdot\text{mol}^{-1}$  for ring-closing of D-glucose

to  $\beta$ -D-glucopyranose (reaction 3) were used without adjustment.  $E_a$  values of  $33.6 \text{ kcal}\cdot\text{mol}^{-1}$  and  $39.5 \text{ kcal}\cdot\text{mol}^{-1}$  for ring-closing of D-glucose to  $\beta$ -D-glucofuranose and ring-opening of  $\beta$ -D-glucofuranose to D-glucose (reactions 12 and 13), respectively, were used, and the same ratio of  $R_{Na^+}$  for ring-opening of  $\beta$ -D-glucofuranose to  $R_{Na^+}$  for ring-closing of D-glucose to  $\beta$ -D-glucofuranose as reported by Mayes et al.<sup>25</sup> was used.  $E_a$  values of  $40.7 \text{ kcal}\cdot\text{mol}^{-1}$  and  $38.2 \text{ kcal}\cdot\text{mol}^{-1}$  for ring-opening of  $\beta$ -D-fructose to D-fructose and ring-closing of D-fructose to  $\beta$ -D-fructose (reactions 21 and 20), respectively, were used.<sup>25</sup> The reported value of 3.07 for  $R_{Na^+}$  of ring-opening of  $\beta$ -D-fructose to  $R_{Na^+}$  of ring-closing of D-fructose was used in the model and applied to ring-opening of  $\beta$ -D-ketohexose and ring-closing of 3-ketohexose.  $R_{Na^+}$  for ring-opening/ring-closing of 2,3-anhydro- $\beta$ -D-glucopyranose and 3-deoxyglycosulose (reactions 57/56) reported by Mayes et al.<sup>25</sup> was utilized and applied to reactions 36/35 and 51/50.

The catalytic role of NaCl in enhancing the formation of char and gaseous species from fast pyrolysis has been extensively reported in the literature.<sup>11,13,14,17-20,28</sup> It is consistent with our experimental results that showed higher yields of char and gaseous species from fast pyrolysis of glucose-based carbohydrates in the presence of NaCl. To capture these effects, char formation in the presence of NaCl is assumed to be 10.0 times as fast as that in the absence of NaCl;  $E_a$  of  $36.5 \text{ kcal}\cdot\text{mol}^{-1}$  and  $A$  of  $6.5 \times 10^{10} \text{ s}^{-1}$  were used for all the char formation reactions involving  $\text{Na}^+$ -complexes in the model (reactions 70-99).

## Conclusions

Product distributions from fast pyrolysis of glucose-based carbohydrates, including glucose, cellobiose, maltohexaose, and cellulose, in the presence of varying amounts of NaCl at  $500^\circ\text{C}$  were studied using a micropyrolyzer system directly connected to product analysis equipment. LVG, 5-HMF, GA, char,  $\text{H}_2\text{O}$ , and  $\text{CO}_2$  are the major products of fast pyrolysis of glucose-based

carbohydrates without or with NaCl present. The same pyrolysis products in different relative amounts were observed, and their quantified yields were reported. Fast pyrolysis of LVG in the presence of NaCl yielded major products of dianhydroglucopyranose, GA, methylglyoxal, acetol, acetaldehyde, char, CO, CO<sub>2</sub> and H<sub>2</sub>O.

The first model, to the best of our knowledge, for fast pyrolysis of glucose-based carbohydrates that incorporates the significant catalytic effects of NaCl at the mechanistic level was developed in this paper, in which the elementary reactions of neutral species were based on our previous mechanistic model of fast pyrolysis of neat glucose-based carbohydrates, the catalytic effects of NaCl on fast pyrolysis relied on Na<sup>+</sup>, and interactions of Na<sup>+</sup> with neutral species, reactions of Na<sup>+</sup>-complexes, and a degradation scheme of LVG were included. The reactions that were affected by NaCl in fast pyrolysis involved dehydration, cyclic/Grob fragmentation, ring-opening/closing, isomerization, and char formation. Rate parameters for elementary steps that were included in the mechanistic model were specified in terms of pre-exponential factors and activation energies. The mechanistic model incorporating the catalytic effects of NaCl tracks 768 reactions of 222 species for fast pyrolysis of cellulose, which included 252 reactions of 150 species comprising the mechanistic model for glucose decomposition in the presence of NaCl. The mechanistic model will be validated and evaluated against the experimental data in Part 2 of this study.

### Acknowledgment

The authors are grateful for financial support by the Department of Energy (DOE) Office of Energy Efficiency and Renewable Energy (EERE) through the Office of Biomass Program, grant number DEEE0003044. The financial support of the National Science Foundation (CBET-1435228) is gratefully acknowledged. Funding from the Institute for Sustainability and Energy at

Northwestern (ISEN) is also gratefully acknowledged. H. Mayes was supported by the DOE Computational Science Graduate Fellowship (CSGF), which is provided under grant number DE-FG02-97ER25308, and the ARCS Foundation Inc., Chicago Chapter. The authors thank Dr. R. Vinu and Abraham J. Yanez-McKay for fruitful discussions and useful suggestions. The authors also thank Prof. Dr. Jianliang Xiao and Dr. Jianjun Wu at University of Liverpool for discussions on catalysis. This contribution was identified by Richard West (Northeastern University) as the Best Presentation in the session “Reaction Path Analysis I” of the 2014 AIChE Annual Meeting in Atlanta, GA.” The authors are grateful to the anonymous reviewers for their constructive suggestions and comments.

### Literature Cited

1. Carpenter D, Westover TL, Czernik S, Jablonski W. Biomass feedstocks for renewable fuel production: A review of the impacts of feedstock and pretreatment on the yield and product distribution of fast pyrolysis bio-oils and vapors. *Green Chem.* 2014;16:384-406.
2. Kunkes EL, Simonetti DA, West RM, Serrano-Ruiz JC, Gärtner CA, Dumesic JA. Catalytic conversion of biomass to monofunctional hydrocarbons and targeted liquid-fuel classes. *Science.* 2008;322:417-421.
3. Vispute TP, Zhang H, Sanna A, Xiao R, Huber GW. Renewable chemical commodity feedstocks from integrated catalytic processing of pyrolysis oils. *Science.* 2010;330:1222-1227.
4. Mettler MS, Vlachos DG, Dauenhauer PJ. Top ten fundamental challenges of biomass pyrolysis for biofuels. *Energy Environ Sci.* 2012;5:7797-7809.
5. Chundawat SPS, Beckham GT, Himmel ME, Dale BE. Deconstruction of lignocellulosic biomass to fuels and chemicals. *Annu Rev Chem Biomol Eng.* 2011;2:121-145.



6. Bridgwater AV. Review of fast pyrolysis of biomass and product upgrading. *Biomass Bioenergy*. 2012;38:68-94.
7. Ruddy DA, Schaidle JA, Ferrell JR, Wang J, Moens L, Hensley JE. Recent advances in heterogeneous catalysts for bio-oil upgrading via "ex situ catalytic fast pyrolysis": Catalyst development through the study of model compounds. *Green Chem*. 2014;16:454-490.
8. Raveendran K, Ganesh A, Khilar KC. Influence of mineral matter on biomass pyrolysis characteristics. *Fuel*. 1995;74:1812-1822.
9. Jensen A, Dam-Johansen K, Wojtowicz MA, Serio MA. TG-FTIR study of the influence of potassium chloride on wheat straw pyrolysis. *Energy Fuels*. 1998;12:929-938.
10. Shimada N, Kawamoto H, Saka S. Different action of alkali/alkaline earth metal chlorides on cellulose pyrolysis. *J Anal Appl Pyrolysis*. 2008;81:80-87.
11. Patwardhan PR, Satrio JA, Brown RC, Shanks BH. Influence of inorganic salts on the primary pyrolysis products of cellulose. *Bioresour Technol*. 2010;101:4646-4655.
12. Scott DS, Paterson L, Piskorz J, Radlein D. Pretreatment of poplar wood for fast pyrolysis: Rate of cation removal. *J Anal Appl Pyrolysis*. 2001;57:169-176.
13. Chen MQ, Wang J, Zhang MX, et al. Catalytic effects of eight inorganic additives on pyrolysis of pine wood sawdust by microwave heating. *J Anal Appl Pyrolysis*. 2008;82:145-150.
14. Nimlos MR, Blanksby SJ, Ellison GB, Evans RJ. Enhancement of 1,2-dehydration of alcohols by alkali cations and protons: A model for dehydration of carbohydrates. *J Anal Appl Pyrolysis*. 2003;66:3-27.

15. Liu D, Yu Y, Hayashi J, Moghtaderi B, Wu H. Contribution of dehydration and depolymerization reactions during the fast pyrolysis of various salt-loaded celluloses at low temperatures. *Fuel*. 2014;136:62-68.
16. Lowary TL, Richards GN. Mechanisms of pyrolysis of polysaccharides - cellobiitol as a model for cellulose. *Carbohydr Res*. 1990;198:79-89.
17. Low MJD, Morterra C. IR studies of carbons —V effects of NaCl on cellulose pyrolysis and char oxidation. *Carbon*. 1985;23:311-316.
18. Park BI, Bozzelli JW, Booty MR. Pyrolysis and oxidation of cellulose in a continuous-feed and -flow reactor: Effects of NaCl. *Ind Eng Chem Res*. 2002;41:3526-3539.
19. Zaror CA, Hutchings IS, Pyle DL, Stiles HN, Kandiyoti R. Secondary char formation in the catalytic pyrolysis of biomass. *Fuel*. 1985;64:990-994.
20. Wang J, Zhang MQ, Chen MQ, et al. Catalytic effects of six inorganic compounds on pyrolysis of three kinds of biomass. *Thermochim Acta*. 2006;444:110-114.
21. Paulsen AD, Mettler MS, Dauenhauer PJ. The role of sample dimension and temperature in cellulose pyrolysis. *Energy Fuels*. 2013;27:2126-2134.
22. Mayes HB, Nolte MW, Beckham GT, Shanks BH, Broadbelt LJ. The alpha-bet(a) of glucose pyrolysis: Computational and experimental investigations of 5-hydroxymethylfurfural and levoglucosan formation reveal implications for cellulose pyrolysis. *ACS Sustainable Chem Eng*. 2014;2:1461–1473.
23. Zhou X, Nolte MW, Mayes HB, Shanks BH, Broadbelt LJ. Experimental and mechanistic modeling of fast pyrolysis of neat glucose-based carbohydrates. 1. Experiments and development of an advanced mechanistic model. *Ind Eng Chem Res*. 2014;53:13274–13289.

24. Zhou X, Nolte MW, Shanks BH, Broadbelt LJ. Experimental and mechanistic modeling of fast pyrolysis of neat glucose-based carbohydrates. 2. Validation and evaluation of the mechanistic model. *Ind Eng Chem Res.* 2014;53:13290–13301.
25. Mayes HB, Nolte MW, Beckham GT, Shanks BH, Broadbelt LJ. The alpha-bet(a) of salty glucose pyrolysis: Computational investigations of 5-hydroxymethylfurfural and levoglucosan formation reveal cellulose pyrolysis catalytic action by sodium ions. *ACS Catal.* 2015;5:192–202.
26. Jensen PA, Frandsen FJ, Dam-Johansen K, Sander B. Experimental investigation of the transformation and release to gas phase of potassium and chlorine during straw pyrolysis. *Energy Fuels.* 2000;14:1280-1285.
27. Quyn DM, Wu HW, Li CZ. Volatilisation and catalytic effects of alkali and alkaline earth metallic species during the pyrolysis and gasification of Victorian brown coal. Part i. Volatilisation of Na and Cl from a set of NaCl-loaded samples. *Fuel.* 2002;81:143-149.
28. Yu Y, Liu D, Wu H. Formation and characteristics of reaction intermediates from the fast pyrolysis of NaCl- and MgCl<sub>2</sub>-loaded celluloses. *Energy Fuels.* 2013;28:245-253.
29. Wornat MJ, Hurt RH, Yang NYC, Headley TJ. Structural and compositional transformations of biomass chars during combustion. *Combust Flame.* 1995;100:133-145.
30. Mayes HB, Tian J, Nolte MW, Shanks BH, Beckham GT, Gnanakaran S, Broadbelt LJ. Sodium ion interactions with aqueous glucose: Insights from quantum mechanics, molecular dynamics, and experiment. *J Phys Chem B.* 2014;118:1990-2000.
31. Zhang Y, Liu C. A new horizon on effects of alkalis metal ions during biomass pyrolysis based on density function theory study. *J Anal Appl Pyrolysis.* 2014;110:297-304.

32. Broadbelt LJ, Pfaendtner J. Lexicography of kinetic modeling of complex reaction networks. *AIChE J.* 2005;51:2112-2121.
33. Vinu R, Broadbelt LJ. A mechanistic model of fast pyrolysis of glucose-based carbohydrates to predict bio-oil composition. *Energy Environ Sci.* 2012;5:9808-9826.
34. Patwardhan PR, Satrio JA, Brown RC, Shanks BH. Product distribution from fast pyrolysis of glucose-based carbohydrates. *J Anal Appl Pyrolysis.* 2009;86:323-330.
35. Kawamoto H, Murayama M, Saka S. Pyrolysis behavior of levoglucosan as an intermediate in cellulose pyrolysis: Polymerization into polysaccharide as a key reaction to carbonized product formation. *J Wood Sci.* 2003;49:469-473.
36. Bai XL, Johnston P, Brown RC. An experimental study of the competing processes of evaporation and polymerization of levoglucosan in cellulose pyrolysis. *J Anal Appl Pyrolysis.* 2013;99:130-136.
37. Bai XL, Johnston P, Sadula S, Brown RC. Role of levoglucosan physiochemistry in cellulose pyrolysis. *J Anal Appl Pyrolysis.* 2013;99:58-65.
38. Bai X, Brown RC. Modeling the physiochemistry of levoglucosan during cellulose pyrolysis. *J Anal Appl Pyrolysis.* 2014;105:363-368.
39. Shoji T, Kawamoto H, Saka S. Boiling point of levoglucosan and devolatilization temperatures in cellulose pyrolysis measured at different heating area temperatures. *J Anal Appl Pyrolysis.* 2014;109:185-195.
40. Franks F, Hall JR, Irish DE, Norris K. The effect of cations on the anomeric equilibrium of D-glucose in aqueous-solutions - a Raman-spectral study. *Carbohydr Res.* 1986;157:53-64.

41. Rasrendra CB, Makertihartha IGBN, Adisasmito S, Heeres HJ. Green chemicals from D-glucose: Systematic studies on catalytic effects of inorganic salts on the chemo-selectivity and yield in aqueous solutions. *Top Catal.* 2010;53:1241.
42. Kulkarni Vishakha S, Butte Kishor D, Rathod Sudha S. Natural polymers—a comprehensive review. *Int J Res Pharm Biomed Sci.* 2012;3:1597-1613.
43. Zhang J, Nolte MW, Shanks BH. Investigation of primary reactions and secondary effects from the pyrolysis of different celluloses. *ACS Sustainable Chem Eng.* 2014;2:2820–2830.
44. Ronsse F, Bai X, Prins W, Brown RC. Secondary reactions of levoglucosan and char in the fast pyrolysis of cellulose. *Environ Prog Sustain Energy.* 2012;31:256-260.
45. Kawamoto H, Morisaki H, Saka S. Secondary decomposition of levoglucosan in pyrolytic production from cellulosic biomass. *J Anal Appl Pyrolysis.* 2009;85:247-251.
46. Nimlos MR, Evans RJ. Study of reaction pathways in levoglucosan pyrolysis by matrix isolation IR spectroscopy. *Abstr Pap Am Chem Soc.* 2002;223:U585-U585.
47. Zhang XL, Yang WH, Blasiak W. Thermal decomposition mechanism of levoglucosan during cellulose pyrolysis. *J Anal Appl Pyrolysis.* 2012;96:110-119.
48. Lin YC, Cho J, Tompsett GA, Westmoreland PR, Huber GW. Kinetics and mechanism of cellulose pyrolysis. *J Phys Chem C.* 2009;113:20097-20107.
49. Assary RS, Curtiss LA. Thermochemistry and reaction barriers for the formation of levoglucosenone from cellobiose. *ChemCatChem.* 2012;4:200-205.
50. Shen DK, Gu S. The mechanism for thermal decomposition of cellulose and its main products. *Bioresour Technol.* 2009;100:6496-6504.

51. Vinu R, Broadbelt LJ. Unraveling reaction pathways and specifying reaction kinetics for complex systems. *Annu Rev Chem Biomol Eng.* 2012;3:29-54.
52. Lynch BJ, Fast PL, Harris M, Truhlar DG. Adiabatic connection for kinetics. *J Phys Chem A.* 2000;104:4811-4815.
53. Armentrout PB, Simons J. Understanding heterolytic bond cleavage. *J Am Chem Soc.* 1992;114:8627-8633.
54. Heaton AL, Armentrout PB. Experimental and theoretical studies of sodium cation interactions with D-arabinose, xylose, glucose, and galactose. *J Phys Chem A.* 2008;112:10156-10167.
55. Koizumi H, Armentrout PB. Collision-induced dissociation and theoretical studies of  $\text{Cu}^+$ -dimethoxyethane complexes. *J Am Soc Mass Spectrom.* 2001;12:480-489.
56. Hupp JT, Weaver MJ. The frequency factor for outer-sphere electrochemical reactions. *J Electroanal Chem.* 1983;152:1-14.
57. Stojanowska G, Jones JM. Influence of minerals and added calcium on the pyrolysis and co-pyrolysis of coal and biomass. *J Energy Inst.* 2005;78:126-138.
58. Su W, Fang M, Cen J, Li C, Luo Z, Cen K. Influence of metal additives on pyrolysis behavior of bituminous coal by TG-FTIR analysis. In: Qi H, Zhao B, eds. *Cleaner combustion and sustainable world*: Springer Berlin Heidelberg; 2013:149-159.
59. Beliy V, Udoratina E. Kinetic study of wood pyrolysis in presence of metal halides. *Cent Eur J Chem.* 2014;12:1294-1303.
60. Dickerson T, Soria J. Catalytic fast pyrolysis: A review. *Energies.* 2013;6:514-538.
61. Yang X, Zhang J, Zhu X. Thermal degradation kinetics of calcium-enriched bio-oil. *AIChE J.* 2008;54:1945-1953.

62. Seshadri V, Westmoreland PR. Concerted reactions and mechanism of glucose pyrolysis and implications for cellulose kinetics. *J Phys Chem A*. 2012;116:11997-12013.
63. Huang J, Liu C, Wei S, Huang X, Li H. Density functional theory studies on pyrolysis mechanism of  $\beta$ -D-glucopyranose. *J Mol Struct Theochem*. 2010;958:64-70.
64. Assary RS, Curtiss LA. Comparison of sugar molecule decomposition through glucose and fructose: A high-level quantum chemical study. *Energy Fuels*. 2011;26:1344-1352.
65. Shen C, Zhang IY, Fu G, Xu X. Pyrolysis of D-glucose to acrolein. *Chin J Chem Phys*. 2011;24:249-252.
66. Cho JM, Davis JM, Huber GW. The intrinsic kinetics and heats of reactions for cellulose pyrolysis and char formation. *ChemSusChem*. 2010;3:1162-1165.

## Table Captions

**Table 1.** Size of the mechanistic model for fast pyrolysis of glucose, cellobiose, maltohexaose, and cellulose with/without NaCl present in terms of the number of species and reactions.

**Table 2.** Rate parameters of reactions of neutral species introduced by LVG decomposition and reactions of  $\text{Na}^+$ -complexes in the presence of NaCl.

## Table Captions in Supporting Information

**Table S1.** Yields (in wt %) of the chemical species arising from fast pyrolysis of glucose in the presence of NaCl at 500 °C.

**Table S2.** Yields (in wt %) of the chemical species arising from fast pyrolysis of cellobiose in the presence of NaCl at 500 °C.

**Table S3.** Yields (in wt %) of the chemical species arising from fast pyrolysis of maltohexaose in the presence of NaCl at 500 °C.

**Table S4.** Yields (in wt %) of the chemical species arising from fast pyrolysis of cellulose in the presence of NaCl at 500 °C.

**Table S5.** Yields (in wt %) of the chemical species arising from fast pyrolysis of levoglucosan in the presence of NaCl at 500 °C.

## Figure Captions in Supporting Information

**Figure S1.** (a) Identity of cellulosic chains based on end-groups and mid-groups, (b) list of 77 low molecular weight species tracked in the model; all the neutral species can bind with  $\text{Na}^+$  to form the corresponding  $\text{Na}^+$ -complexes.



### Scheme Captions

**Scheme 1.** Modeling approach to capture the effects of  $\text{Na}^+$  on the product distribution involved adding interactions of  $\text{Na}^+$  with cellulose and its derivative polymer chains (*e.g.*, cellulose chain, NR-end chain, and LVG-end chain) and adding parallel reaction pathways (*e.g.*, dehydration) mediated by  $\text{Na}^+$  with different kinetic parameters.

**Scheme 2.** Modeling approach to capture the effects of  $\text{Na}^+$  on the product distribution involved adding interactions of  $\text{Na}^+$  with low molecular weight species (*e.g.*, glucose and levoglucosan) and adding parallel reaction pathways (*e.g.*, dehydration) mediated by  $\text{Na}^+$  with different kinetic parameters.

**Scheme 3.** Degradation mechanism of levoglucosan during fast pyrolysis in the presence of NaCl. The dehydrated species can undergo char formation to give char, CO,  $\text{CO}_2$ ,  $\text{H}_2\text{O}$ , and  $\text{H}_2$ .

### Scheme Captions in Supporting Information

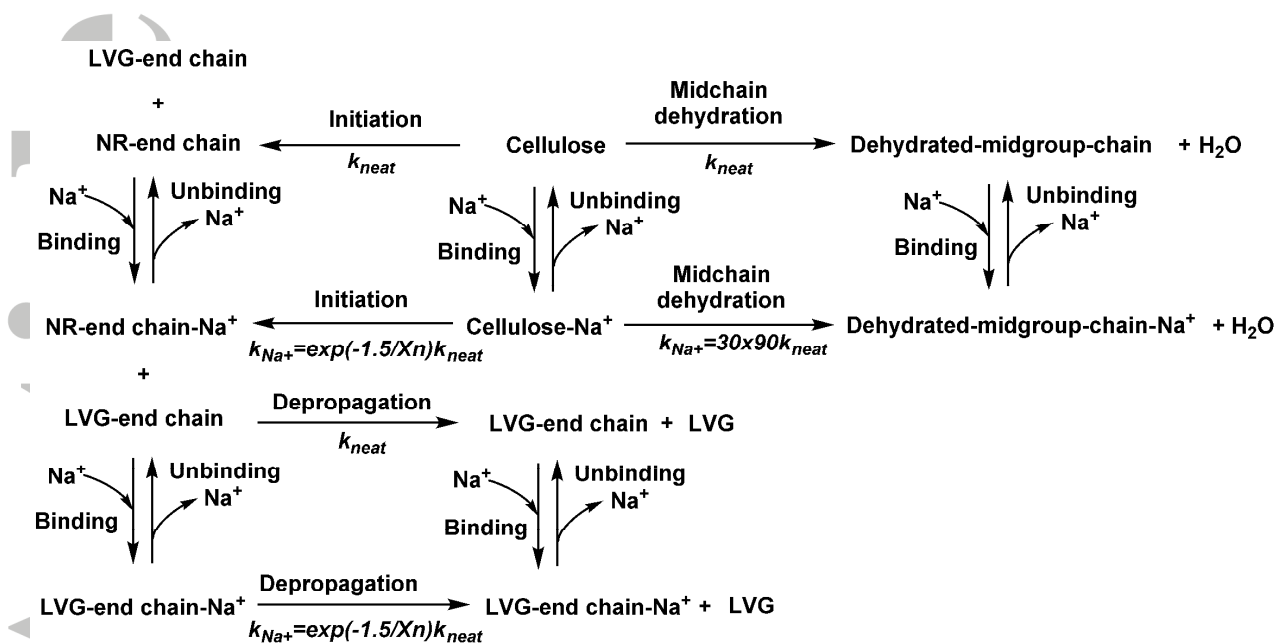
**Scheme S1.** Decomposition mechanisms of cellulose/maltohexaose chains involving end-groups.

**Scheme S2.** Decomposition mechanisms of cellulose/maltohexaose chains involving mid-groups.

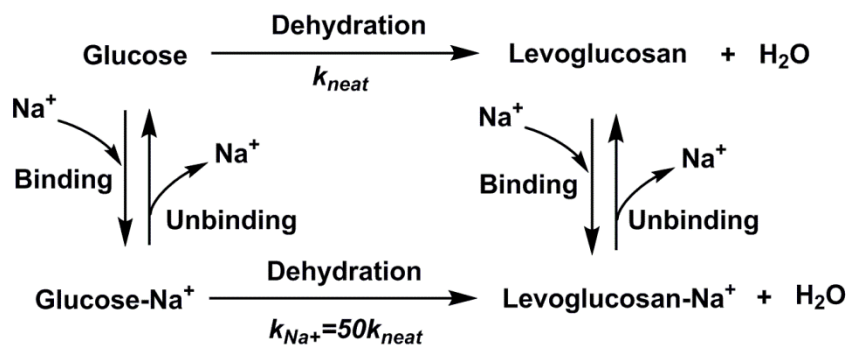
**Scheme S3.** Reaction mechanism of  $\beta$ -D-glucopyranose to form a variety of C1-C6 compounds during fast pyrolysis.

**Scheme S4.** Continued mechanism of the formation of C1-C6 compounds.

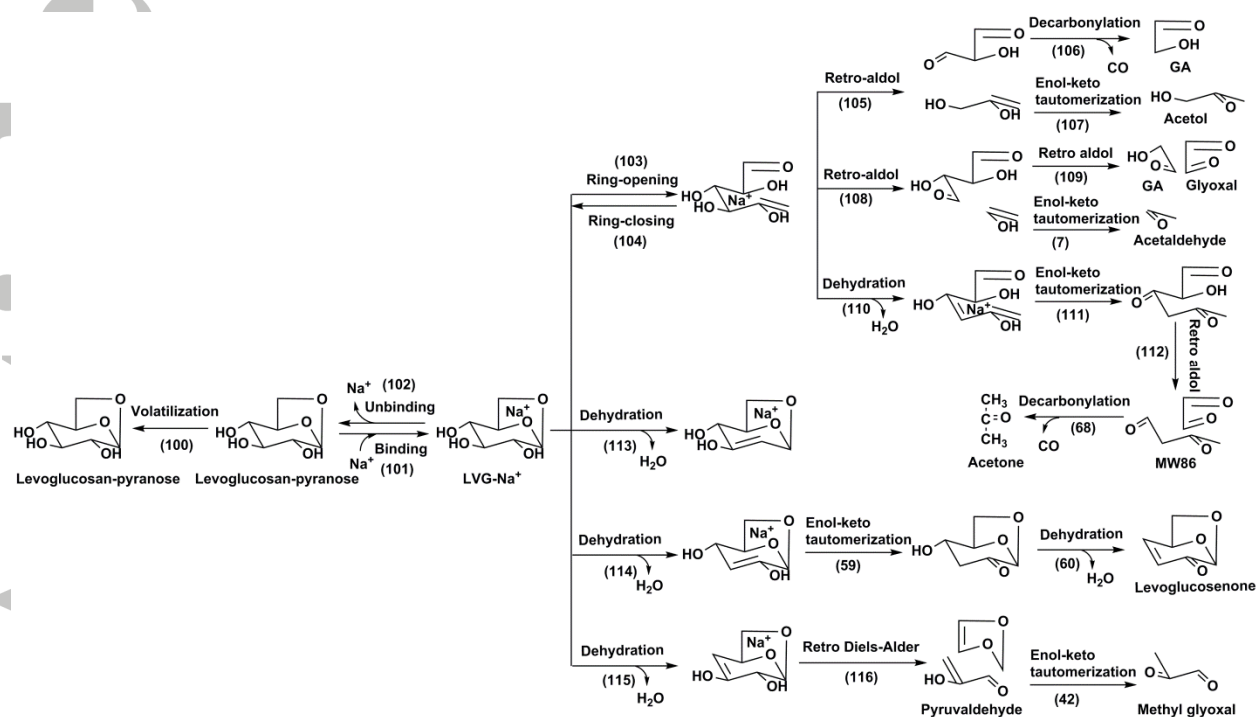
**Scheme S5.** Char formation of various dehydrated species.



**Scheme 1.** Modeling approach to capture the effects of  $\text{Na}^+$  on the product distribution involved adding interactions of  $\text{Na}^+$  with cellulose and its derivative polymer chains (*e.g.*, cellulose chain, NR-end chain, and LVG-end chain) and adding parallel reaction pathways (*e.g.*, dehydration) mediated by  $\text{Na}^+$  with different kinetic parameters.



**Scheme 2.** Modeling approach to capture the effects of  $\text{Na}^+$  on the product distribution involved adding interactions of  $\text{Na}^+$  with low molecular weight species (*e.g.*, glucose and levoglucosan) and adding parallel reaction pathways (*e.g.*, dehydration) mediated by  $\text{Na}^+$  with different kinetic parameters.



**Scheme 3.** Degradation mechanism of levoglucosan during fast pyrolysis in the presence of NaCl. The dehydrated species can undergo char formation to give char, CO, CO<sub>2</sub>, H<sub>2</sub>O, and H<sub>2</sub>.

**Table 1.** Size of the mechanistic model for fast pyrolysis of glucose, cellobiose, maltohexaose, and cellulose with/without NaCl present in terms of the number of species and reactions.

reactant	no. of species		no. of reactions	
	neat	with NaCl	neat	with NaCl
glucose	67	150	96	252
cellobiose	79	174	137	356
maltohexaose	103	222	342	768
cellulose	103	222	342	768

**Table 2.** Rate parameters of reactions of neutral species introduced by LVG decomposition and reactions of  $\text{Na}^+$ -complexes in the presence of NaCl.

reaction type	reaction index <sup>a</sup>	$A, \text{s}^{-1}$ or $\text{M}^{-1}\text{s}^{-1}$	$E_a,$ $\text{kcal}\cdot\text{mol}^{-1}$	ref. $A$	ref. $E_a$
volatilization	100	3		fit	
binding	101	$1.00 \times 10^8$	0	56	54
unbinding <sup>b</sup>	102	$7.05 \times 10^8$	—	25	54
retro-aldol	105,	$2.29 \times 10^{12}$	36.5	62	62
	108, 109, 112	$1.00 \times 10^{12}$	39.7	62	62
decarbonylation	106	$5.00 \times 10^{15}$	62.0	23	63
enol-keto tautomerization	7, 107, 111	$5.00 \times 10^{15}$	57.0	62	62
dehydration	110	$2.00 \times 10^{15}$	50.5	22	22
retro Diels–Alder	116	$1.07 \times 10^{15}$	55.0	64	64
dehydration catalyzed by $\text{Na}^+$	V, 1	$2.02 \times 10^{14}$	47.4	25	25
	VI, viii, 4	$2.31 \times 10^{15}$	56.0	25	25
	i, iv,	$5.00 \times 10^{15}$	53.1	23	fit
	X, 8	$2.00 \times 10^{15}$	46.0	23	fit

Accepted Article

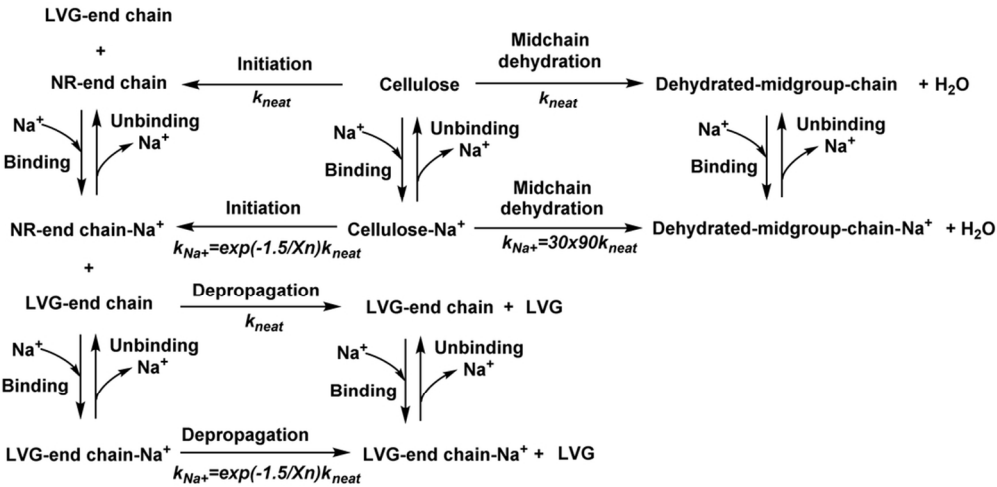
	14	$6.50 \times 10^{14}$	49.2	25	25
	22	$2.50 \times 10^{15}$	51.6	25	25
	23, 31, 37, 52	$9.06 \times 10^{12}$	38.3	25	25
	24	$5.00 \times 10^{15}$	50.5	25	25
	32, 38	$5.00 \times 10^{15}$	53.0	25	25
	45	$1.00 \times 10^9$	25.9	65	fit
	53	$5.00 \times 10^{15}$	56.5	25	25
	55, 63, 64, 110	$2.00 \times 10^{15}$	47.8	65	fit
	58	$3.00 \times 10^{13}$	44.1	49	fit
	60	$5.00 \times 10^{12}$	44.1	49	fit
	113, 114, 115	$5.25 \times 10^{15}$	50.0	25	25
ring-opening/closing catalyzed by Na <sup>+</sup>	2, 103	$1.00 \times 10^{15}$	46.3	25	25
	3, 104	$1.10 \times 10^{12}$	37.8	25	25
	12	$4.12 \times 10^{11}$	33.6	25	25
	13	$9.00 \times 10^{13}$	39.5	25	25
	20	$2.00 \times 10^{12}$	38.2	25	25
	21	$4.00 \times 10^{13}$	40.7	25	25

	28	$6.65 \times 10^{11}$	31.7	25	25
	29	$6.65 \times 10^{14}$	41.7	25	25
	35, 50	$1.28 \times 10^{12}$	37.6	25	25
	36, 51	$4.39 \times 10^{13}$	42.1	25	25
	56	$2.15 \times 10^{13}$	42.0	25	25
	57	$1.23 \times 10^{14}$	46.0	25	25
isomerization catalyzed by $\text{Na}^+$	19	$1.50 \times 10^{12}$	36.5	25	25
cyclic/Grob fragmentation by $\text{Na}^+$	15, 30	$8.00 \times 10^{14}$	49.0	65	fit
	33, 39	$1.50 \times 10^{15}$	49.0	65	fit
char formation catalyzed by $\text{Na}^+$	70–99	$6.50 \times 10^{10}$	36.5	66	fit

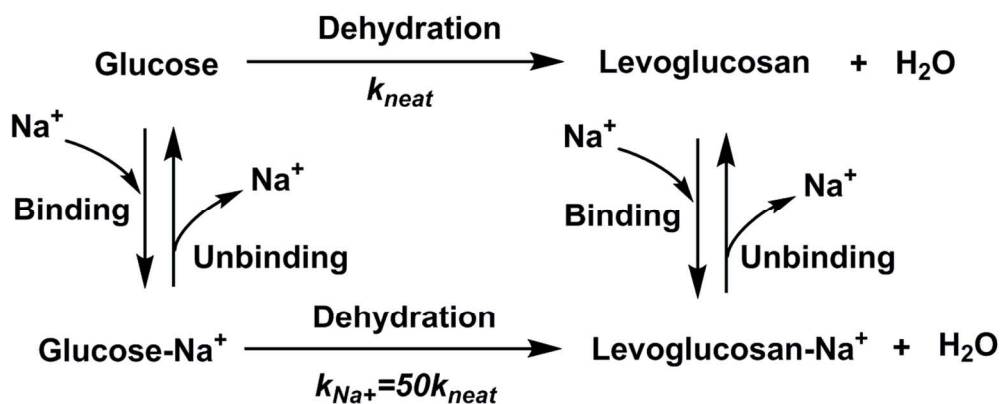
<sup>a</sup> Reaction indices refer to reactions in Scheme 3 and Schemes S1–S5. <sup>b</sup> The rate coefficient for unbinding was calculated based on the free energy of reaction and the rate coefficient for binding. The value given for A is equal to k at 773.15 K.



Accepted



95x46mm (300 x 300 DPI)



111x46mm (300 x 300 DPI)



AIChE Journal